SCIEPublish

Article

A Novel Prognostic Model for DLBCL Patients Based on Cuproptosis-Related Genes

Fu Li [1,†], Jiao Cai [2,3,†], Jiali Li [1], Jun Rao [1], Song Dong [1], Shijia Lin [1], Xixi Xiang [1], Xi Zhang [1,*] and Li Gao [1,*]

[1] Medical Center of Hematology, Xinqiao Hospital, Army Medical University, Chongqing 400037, China; 335984186@qq.com (F.L.); kll6324@163.com (J.L.); raojun1129@126.com (J.R.); dongsonne@yeah.net (S.D.); linshijiajia@163.com (S.L.); xixixiangcici@outlook.com (X.X.)

[2] Department of Hematology and Hematopoietic Stem Cell Transplantation Centre, General Hospital of Western Theater Command, Chengdu 610083, China; 2432556899@qq.com (J.C.)

[3] Department of Stem Cell and Regenerative Medicine, Southwest Hospital, Army Medical University, Chongqing 400038, China

* Corresponding author. E-mails: zhangxxi@sina.com (X.Z.); gaotiantiantiger@163.com (L.G.)

† These authors contributed equally to this work.

Received: 10 August 2023; Accepted: 22 January 2024; Available online: 30 June 2024

ABSTRACT: The current classification system for diffuse large B-cell lymphoma (DLBCL) cannot fully explain prognostic differences in DLBCL patients. Cuproptosis is a newly discovered programmed cell death which depends on copper ions. In this study, a prognostic model based on cuproptosis-related genes was constructed using a public database. COX regression analysis was performed on training set-GSE31312 to construct a prognostic model based on cuproptosis-related genes, and the validation set-GSE181063 was used to verify the prognostic model. Gene Set Enrichment Analysis (GSEA) was used to explore the underlying mechanism behind differences in the prognosis of DLBCL patients. Finally, molecular docking was used to screen out compounds that may act on cuproptosis-related genes. A prognostic model based on 5 cuproptosis-related genes was constructed (*CDKN2A*×1.547905713-*DLAT*×2.241073725-*DLD*×1.907442964-*LIPT1*×2.689158994-*MTF1*×2.069682266) from training set-GSE31312. According to this model, DLBCL patients were divided into high-risk and low-risk groups. The survival time of high-risk patients was significantly shorter than that of the low-risk group ($p = 2.636 \times 10^{-7}$). In the validation set-GSE181063, the survival time of the high-risk group was also shorter than that of the low-risk group ($p = 2.462 \times 10^{-3}$). Among the 5 cuproptosis-related genes, only *CDKN2A* played a tumorigenesis role. Finally, three small molecule compounds with the lowest *CDKN2A* binding energy were found by virtual docking: irinotecan, lumacaftor and nilotinib, which may be used as potential targeted drugs. A prognostic model based on 5 cuproptosis-related genes was constructed in this study, and 3 potential targeted inhibitors of *CDKN2A* were screened out by molecular docking.

Keywords: DLBCL; Cuproptosis; Prognostic model; COX regression

1. Introduction

Diffuse large B-cell lymphoma (DLBCL), the most common non-Hodgkin's lymphoma (NHL), is a highly heterogeneous and invasive cancer [1]. The current standard treatment for DLBCL is R-CHOP, a combination of rituximab with cyclophosphamide, adriamycin, vincristine and prednisone [2]. R-CHOP is effective for most DLBCL patients; however, 30%–40% of patients with refractory or relapse still have a poor prognosis [3]. The International Prognostic Index (IPI) is the most commonly used prognostic indicator for DLBCL patients. It is composed of common clinical features, including the Eastern Cooperative Oncology Group (ECOG) score, age, stage, extranodal lesions, and lactate dehydrogenase [4]. Cell origin classification (COO) can classify DLBCL into two main subtypes, namely germinal center B cell (GCB) and non-germinal center B cell (non-GCB) [5]. Compared with GCB subtype, non-GCB DLBCL patients have stronger invasion, higher drug resistance, higher recurrence rate and worse prognoses [6]. Based

https://doi.org/10.70322/BG20240110002

on the immunohistochemistry and FISH results of BCL2, BCL6, and MYC, "double-protein" and "double-hit" or "triple-hit" types can be identified as having worse prognoses [7,8]. In addition, LymphGen Genetic Subtype Classifier, which is a widely used gene expression based prognostic classifier in clinic, divides DLBCL patients into seven subtypes: MCD, N1, A53, BN2, ST2, EZB/MYC$^+$, and EZB/MYC$^-$ [1]. However, the above prognosis prediction, which is based on clinical characteristics, cell origin and gene expression, cannot fully explain the heterogeneity in DLBCL patients [9,10].

Recently, Peter et al. discovered cuproptosis, a new regulated cell death pattern that depends on copper ions, which is different from apoptosis, iron death and necrosis [11]. Copper ions directly bind to the lipoacylated components of tricarboxylic acid cycle (TCA) which leads to abnormal aggregation of lipoacylated proteins and loss of iron-sulfur cluster proteins, resulting in protein toxic stress and cell death [11]. In addition, the study found that seven genes (*FDX1*, *LIAS*, *LIPT1*, *DLD*, *DLAT*, *PDHA1*, and *PDHB*) inhibited cuproptosis, while three genes (*MTF1*, *GLS*, and *CDKN2A*) promoted it [11]. As a newly discovered pattern of regulated cell death, there have been studies showing that cuproptosis plays an important role in lung cancer, hepatocellular carcinoma, melanoma and other tumors [12–14]. However, the role of cuproptosis and cuproptosis-related genes in tumorigenesis, development, and prognosis remains unclear for DLBCL patients.

Therefore, this study explored the effects of cuproptosis-related genes on the prognosis of DLBCL patients by analyzing the DLBCL dataset from the public database. A prognostic model based on cuproptosis-related genes was constructed, hoping to provide a new idea for the treatment and prognosis evaluation of DLBCL patients.

2. Materials and Methods

2.1. Datasets

Ten cuproptosis-related genes (*FDX1*, *LIAS*, *LIPT1*, *DLD*, *DLAT*, *PDHA1*, *PDHB*, *MTF1*, *GLS*, and *CDKN2A*) were derived from the study of Peter et al. [11]. Two datasets related to this study were obtained from the GEO database (https://www.ncbi.nlm.nih.gov/geo/). Then, the gene expression value was normalized by RMA function. GSE31312 (https://www.ncbi.nlm.nih.gov/geo/query/acc.cgi?acc=GSE31312) dataset, containing 498 DLBCL patients who were newly diagnosed between January 2002 and October 2009, was generated using the GPL570 (Affymetrix Human Genome U133 Plus 2.0 Array) platform. All patients were treated with R-CHOP, while only 475 patients' clinical information was available. After removing 5 patients without a GSM code, 470 samples were enrolled in the following study. GSE181063 dataset consists of 1310 samples diagnosed between 1 September 2004 and 31 August 2012, which was generated using the GPL14951 (Illumina Human HT-12 WG-DASL V4.0 R2 expression bead chip). GSE181063 (https://www.ncbi.nlm.nih.gov/geo/query/acc.cgi?acc=GSE181063) dataset contains 1149 DLBCL, 21 DLBCL-HL, 83 Burkitt, 40 Hodgkin, 1 LPD-NOS, 1 MGUS, 15 Plasmacytoma, and 1042 DLBCL In this study, 765 of the 1042 DLBCL patients treated with R-CHOP were enrolled. The patients' clinical information was summarized in Table 1.

Table 1. Clinical information of patients.

Characteristics	GSE31312 Cohort	GSE10846 Cohort
No. of patients	470	765
Age, year		
>60	270	538
≤60	200	227
Gender		
Female	199	364
Male	271	401
Stage		
I/II	220	257
III/IV	229	425
Unknown	21	83
IPI score		
0	44	50
1	125	123
2	105	164
3	92	150
4	51	84
5	7	13
Unknown	46	182
Subtype		
GCB	227	360
non-GCB	243	405
Survival status		
Dead	170	351
Alive	300	414

2.2. Unsupervised Cluster

Unsupervised clustering analysis, namely hierarchical cluster analysis, was performed through R package "ConsensusClusterPlus", and visualized by heatmap. Pearson correlation coefficient [15], average linkage [16] and hierarchical clustering method [17] were adopted for cluster analysis. GSE31312 patients were clustered by the expression of cuproptosis-related genes.

2.3. Immune Infiltration Analysis

GSE31312 was utilized for immune infiltration analysis. The CIBERSORT algorithm was employed to estimate the infiltration of immune cells in cluster1 and cluster2 [18]. The results were visualized by heatmap. The boxplot displayed the proportion of 22 immune cell types in cluster1 and cluster2.

2.4. Functional Enrichment Analysis

GSEA (V4.1.0) software was employed to compare the difference of mechanism between cluster1 and cluster2. Gene Ontology (GO) and Kyoto Encyclopedia of Genes and Genomes (KEGG) pathway analyses were performed [19–21]. Physiological functions, including cellular component (CC), molecular function (MF), and biological process (BP), were incorporated in the GO analysis. The items with $p < 0.05$ in the Benjamini-Hochberg test were considered statistically significant.

2.5. Construction of Prognostic Models

Univariate COX regression analysis was used to screen cuproptosis-related genes that significantly affected the prognosis of DLBCL patients, and then multivariate COX regression was used to construct a prognosis model based on cuproptosis-related genes. Finally, the model was verified by GSE181063.

2.6. Nomogram Model

Univariate and multivariate regression analyses were performed to screen for independent prognostic factors in patients' clinical characteristics and the cuproptosis-related model ($p < 0.05$). A Nomogram model was constructed by integrating independent prognostic factors using RMS package (v6.2-0).

2.7. Molecular Docking

The protein structures of cuproptosis-related genes were downloaded through the PDB database (https://www.rcsb.org/), and dehydrate and hydrogenate protein structures were downloaded through PyMOL (v2.4.1) and AutoDock tools (v1.5.6). The binding pocket of the protein was predicted through proteins.plus (https://proteins.plus/), and then the size and coordinates of the pocket were calculated through autodock tools (v1.5.6). A total of 2115 FDA approved small molecule compounds were downloaded from the ZINC15 website (https://zinc.docking.org/substances/subsets/fda/). Finally, AutoDock Vina (v1.2.0) was used to dock the protein structures of cuproptosis-related genes and small molecular compounds to obtain their respective binding energies.

3. Results

3.1 DLBCL Patients Were Clustered According to the Expression of Cuproptosis-Related Genes

To explore the prognostic value of cuproptosis genes in DLBCL and its potential mechanism, public data were used. The specific process is shown in Figure 1.

A total of 470 DLBCL patients in the GSE31312 dataset were clustered by unsupervised clustering on the basis of the expression of 10 cuproptosis-related genes. As shown in Figure 2A, the patients were divided into two clusters (cluster1 and cluster2). The heatmap showed that there were significant differences in gene expression between different clusters (Figure 2B). Principal component analysis (PCA) indicated that DLBCL patients were well distributed into two categories (Figure 2C). Further survival analysis found that there was a significant difference in the overall survival (OS) between the two clusters ($p = 1.62 \times 10^{-6}$) (Figure 2D).

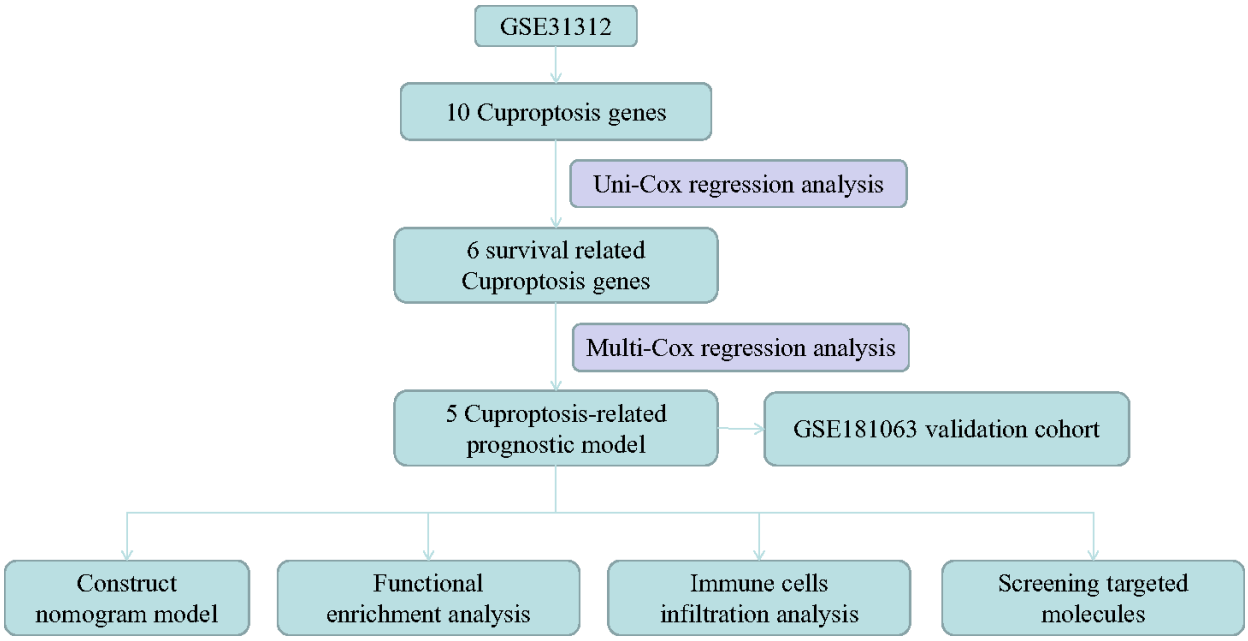

Figure 1. Flowchart of the process in this study.

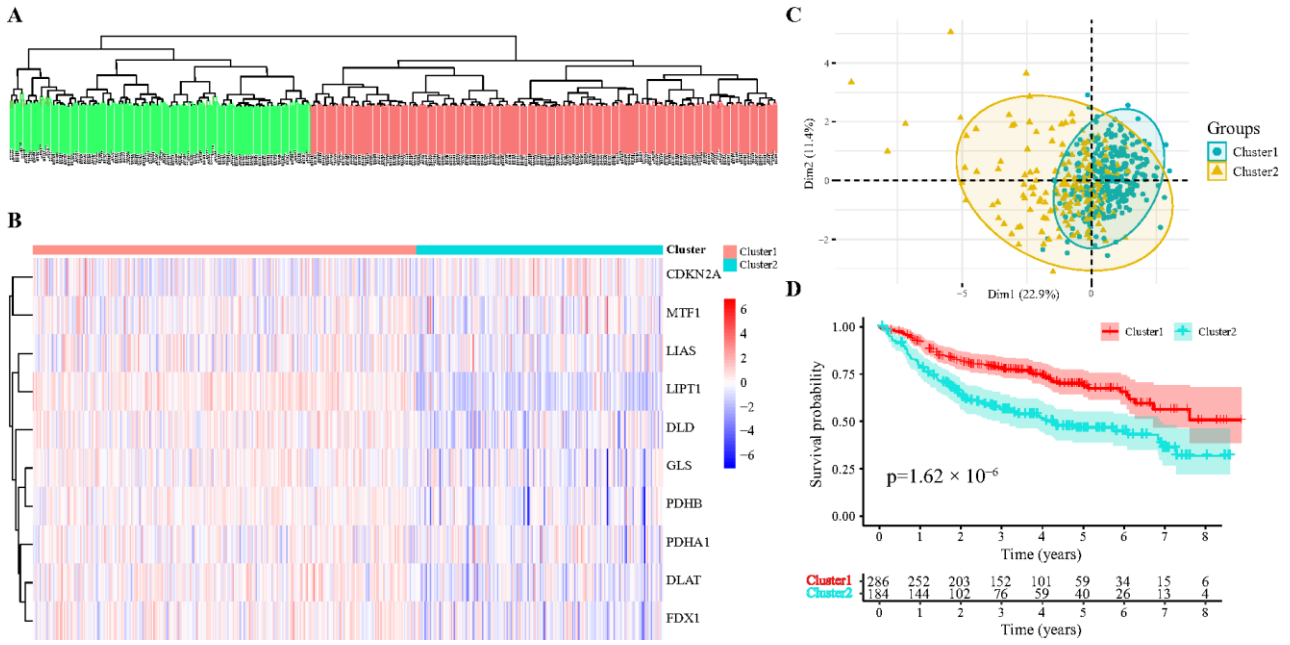

Figure 2. Unsupervised cluster. (**A**): 470 patients of GSE31312 were clustered into cluster1 and cluster2 according to 10 cuproptosis-related genes. (**B**): The expression heatmap of the cuproptosis-related genes in cluster1 and cluster2. (**C**): PCA distribution of cluster1 and cluster2. (**D**): Survival analysis between cluster1 and cluster2 ($p = 1.62 \times 10^{-6}$).

3.2. The Construction of Prognosis Model

Univariate Cox regression analysis of 10 cuproptosis-related genes showed that 6 genes significantly affected the prognosis of DLBCL patients (Table 2). These 6 cuproptosis-related genes were used for multivariate Cox regression analysis to build a prognosis model. Finally, *PDHB* was excluded from the model, and a prognostic model based on Cuproptosis-related Signature (CRS) and composed of five cuproptosis-related genes (*CDKN2A*×1.547905713-*DLAT*×2.241073725-*DLD*×1.907442964-*LIPT1*×2.689158994-*MTF1*×2.069682266) was obtained.

According to the model score, the patients were divided into high-risk ($n = 111$) and low-risk groups ($n = 112$). The two groups' survival analysis showed that the prognosis of high-risk and low-risk patients was significantly different ($p = 2.636 \times 10^{-7}$) (Figure 3A,C,D). The efficiency of the prognostic model was judged by ROC curve, where AUC = 0.7 (1 year), 0.7 (3 years), 0.65 (5 years) (Figure 3B), indicating that the prediction efficiency of the model was good.

GSE181063 dataset ($n = 765$) was used to verify the above prognostic model. Survival analysis showed that the model could effectively distinguish patients into high-risk and low-risk groups ($p = 2.462 \times 10^{-3}$) (Figure S1).

Table 2. Univariate Cox regression analysis of 10 cuproptosis-related genes.

Symbol	HR	HR.95L	HR.95H	*P* value
LIPT1	0.031892	0.0078	0.130396	1.62E-06
DLAT	0.039307	0.008458	0.18268	3.65E-05
DLD	0.042221	0.008651	0.206068	9.12E-05
PDHB	0.05484	0.009328	0.322407	0.001316
CDKN2A	4.767629	1.119743	20.29955	0.034603
MTF1	0.072192	0.005988	0.870314	0.038516
LIAS	0.290913	0.065003	1.301945	0.106339
FDX1	0.268458	0.042605	1.69159	0.16144
PDHA1	0.511945	0.027499	9.530951	0.65359
GLS	0.651152	0.057746	7.342421	0.728536

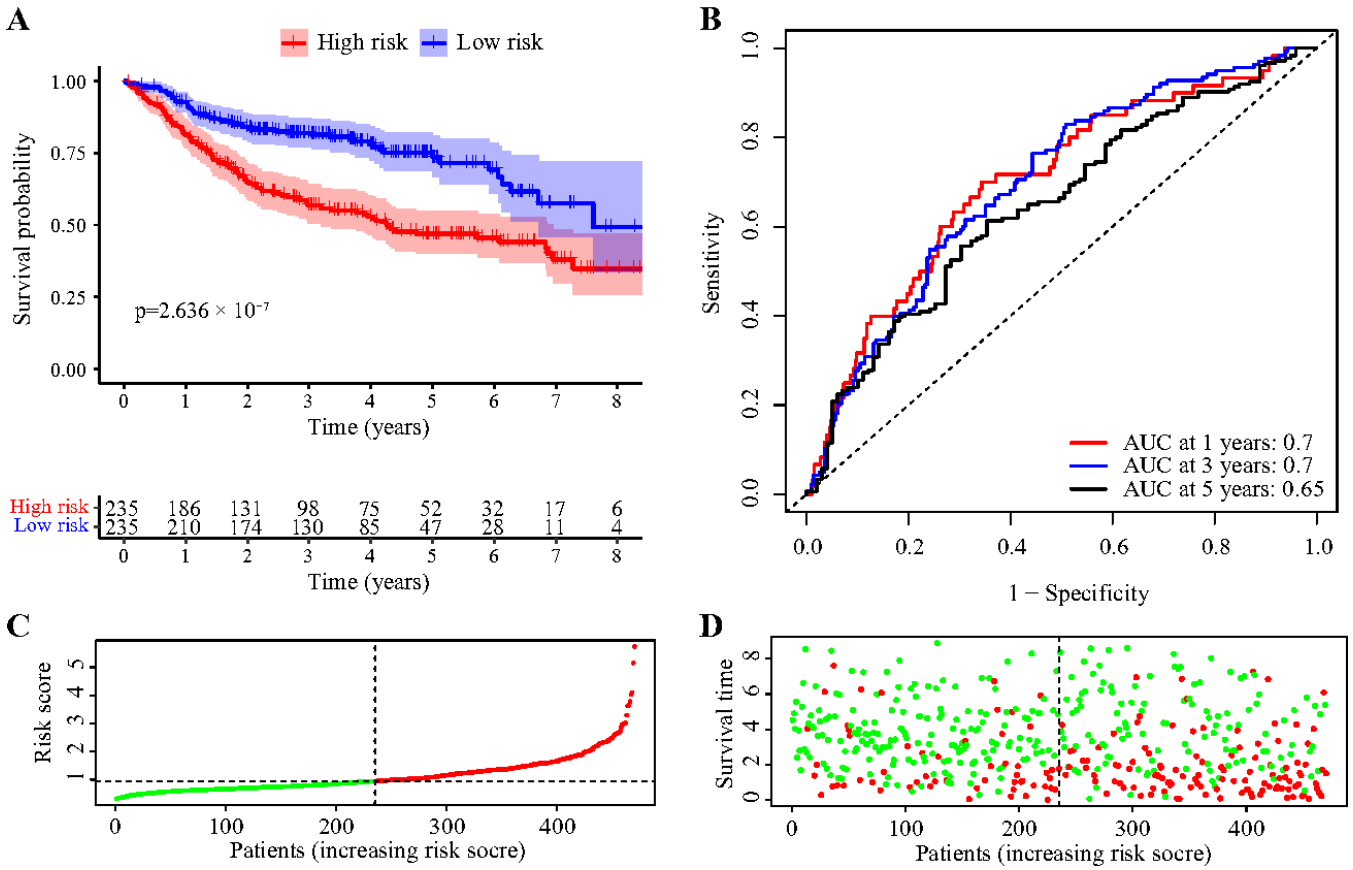

Figure 3. Risk score model based on 5 prognostic related Cuproptosis Genes in GSE31312. (**A**): Kaplan–Meier curves of OS in high-risk and low-risk groups. (**B**): Time-dependent ROC curves for 0, 1, 3, 5 years. The distribution of the risk score (**C**) and survival time (**D**) in 470 DLBCL patients, with a median of 0.945 selected as the cutoff.

3.3. Predictive Stability Analysis of Prognostic Model

After the 470 patients were grouped according to clinical characteristics (Ann Arbor Stage, Age, B-Symptom, Bulky, COO, ECOG, Gender, IPI, and LDH), the survival analyses of patients in high-risk and low-risk groups was carried out respectively. The results showed that the model could still predict the prognosis of patients effectively ($P < 0.0001$) (Figure S2).

3.4. The Construction of Nomogram

Univariate Cox analysis of clinical characteristics (Gender, IPI, B-symptom, COO, and Bulky) and CRS of DLBCL patients showed that IPI, COO, and CRS could significantly affect the prognosis of DLBCL patients (Figure 4A). Multivariate Cox regression analysis of the above prognostic factors revealed that IPI, COO and CRS were independent prognostic factors of DLBCL patients (Figure 4B). The IPI, COO, and CRS were combined to construct a nomogram prognostic model (Figure 4C). The ROC curve (Figure 4D) and calibration curve (Figure 4E–G) suggested that this model was effective.

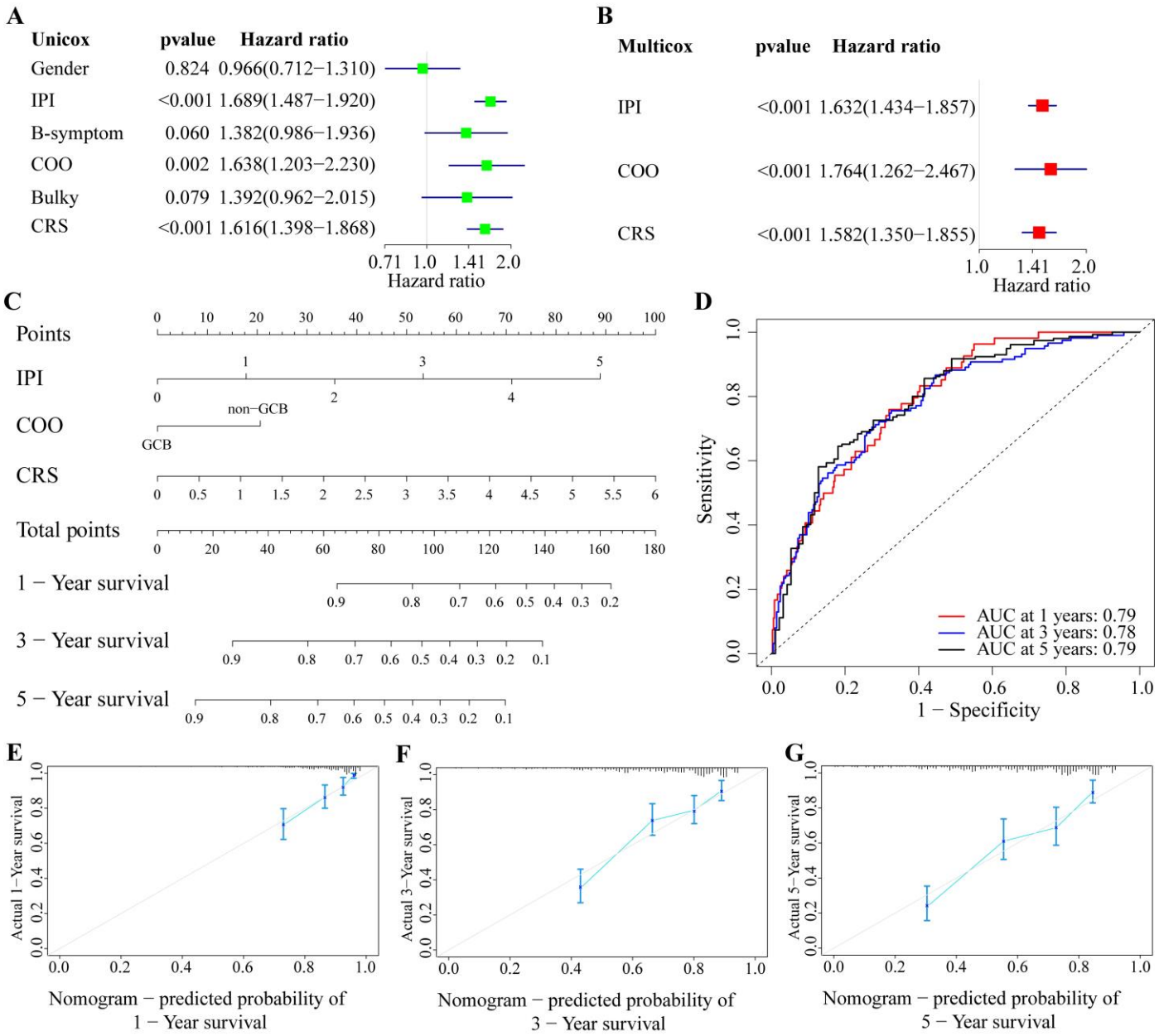

Figure 4. Nomogram based on CRS and clinical factors. (**A**): The univariate Cox regression analyses of Gender, IPI, B-symptom, COO, Bulky and CRS. (**B**): The multivariate Cox regression analyses of IPI, COO, and CRS. (**C**): Nomogram for predicting 1-, 3-, and 5-year OS. (**D**): Time-dependent ROC curves for 0, 1, 3, 5 years. (**E**–**G**). Calibration curves predicted and observed 1-, 3-, and 5-year survival nomogram consistency.

3.5. Functional Enrichment Analysis

The biological function differences between DLBCL patients in high-risk and low-risk groups were analyzed by GSEA. The late endosome to vacuole transport (GOBP) (Figure 5A) enriched in the high-risk group. The mRNA transcription (GOBP) (Figure 5B) and drug metabolism-other enzymes (KEGG) (Figure 5C) enriched in the low-risk group ($P < 0.01$, FDR < 0.25).

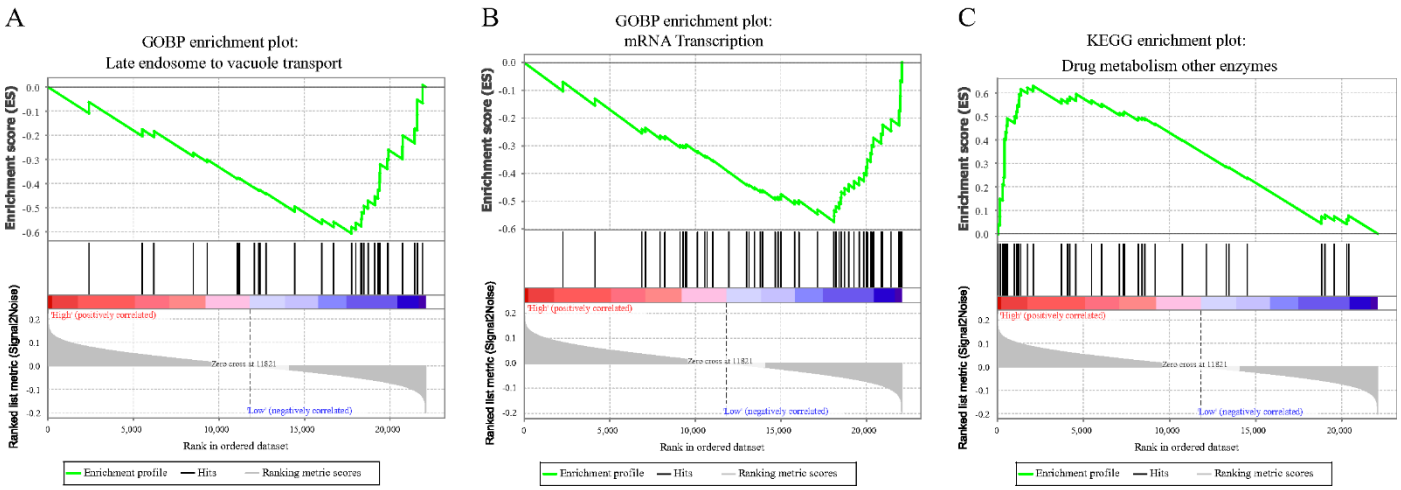

Figure 5. GSEA analysis between high-risk and low-risk groups. (**A**): The late endosome to vacuole transport enriched in the high-risk group. (**B**): The mRNA transcription enriched in the low-risk group. (**C**): The drug metabolism-other enzymes enriched in the low-risk group.

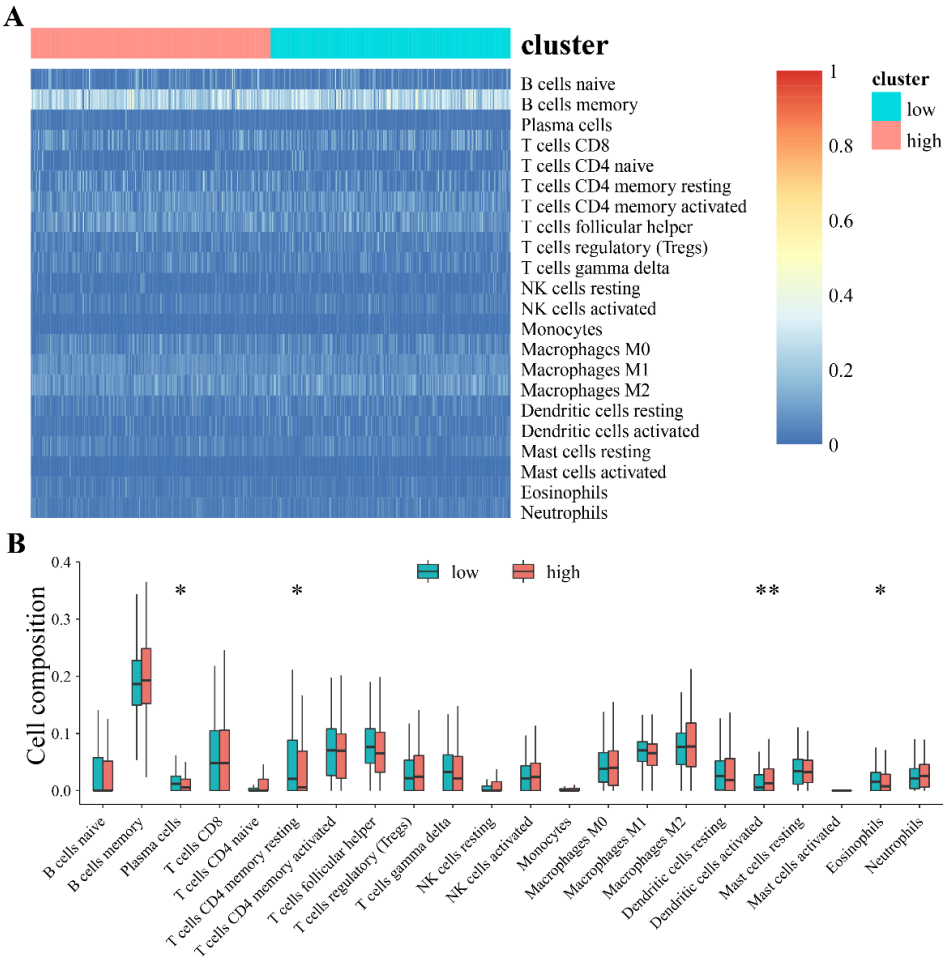

Figure 6. Immune cell infiltration (**A**) and the distribution of specific cells (**B**) in DLBCL patients between the high-risk group and the low-risk group. * $P < 0.05$, ** $P < 0.01$.

3.6. Analysis of Immune Infiltration between Subtypes

CIBERSORT was used to analyze the immune cell infiltration of DLBCL patients. It can be seen that there is no significant difference in the degree of immune infiltration between high-risk and low-risk groups from the heatmap (Figure 6A). The distribution of specific cells was further explored between patients in high-risk and low-risk groups through the box plots. Plasma cells, memory-resting $CD4^+$ T cells, and eosinophils were highly expressed in the low-risk group ($P < 0.05$), and activated dendritic cells were highly expressed in the high-risk group ($P < 0.01$) (Figure 6B).

3.7. Screening Targeted Small Molecule Compounds

Among the 5 cuproptosis-related genes, *CDKN2A* showed a significant facilitating effect on DLBCL. Therefore, this study hopes to screen possible targeted inhibitors of *CDKN2A* through molecular docking. The protein structure of *CDKN2A* was obtained from the PDB database. The proteins.plus website was employed to predict the most likely binding *CDKN2A* pocket (Figure 7A), which was selected for subsequent molecular docking. The 2115 FDA approved compounds were obtained from the ZINC15 database, which were docked with *CDKN2A* to identify compounds with the lowest binding energy. It was found that three compounds (non-psychoactive) with the lowest binding energy to *CDKN2A* were irinotecan, lumacaftor, and nilotinib (Figure 7B–D). Subsequently, our team will verify the effects of these three drugs on DLBCL *in vitro* and *in vivo* to guide clinical practice.

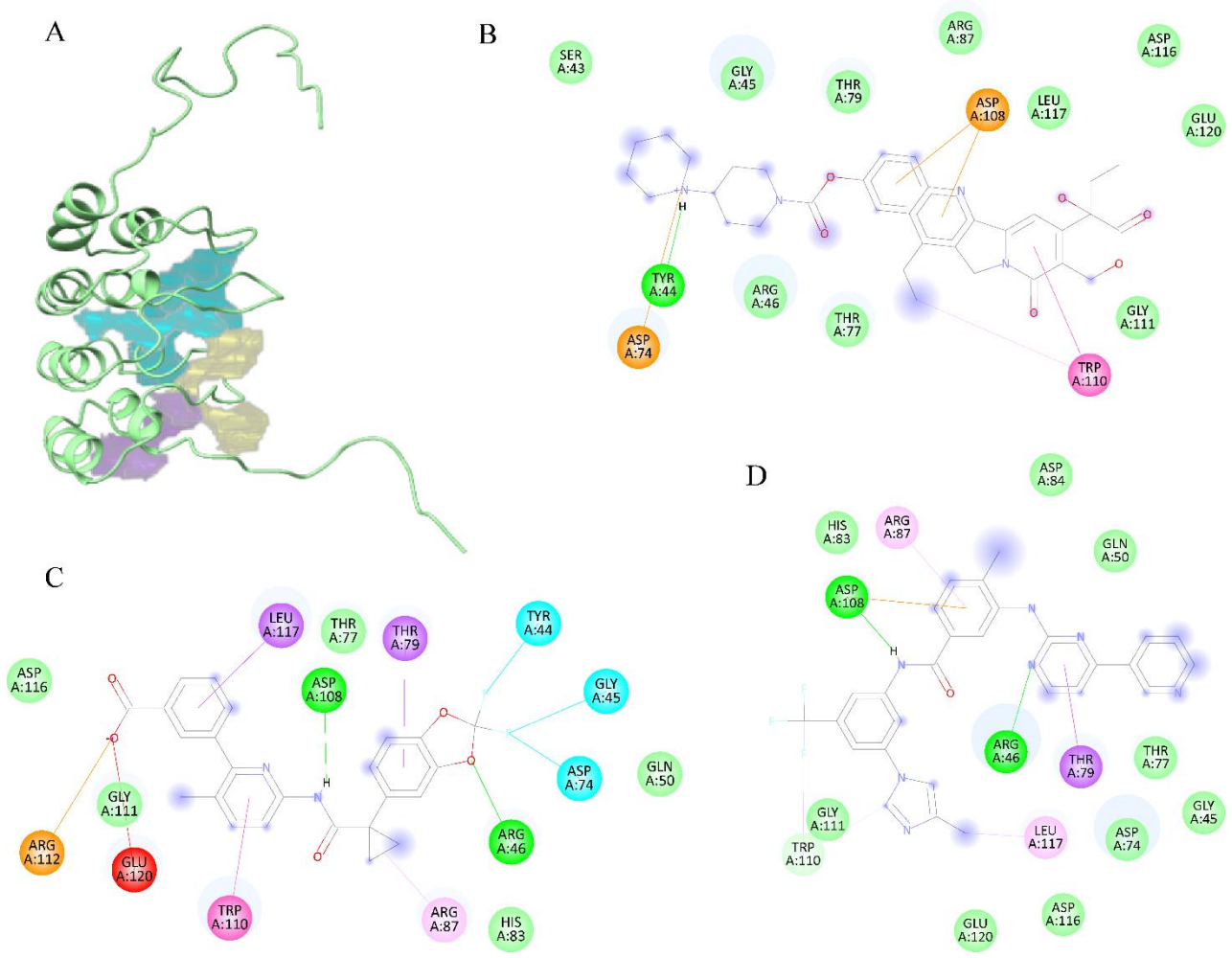

Figure 7. Molecular docking of *CDKN2A*. (**A**): The protein structure of *CDKN2A* and three predicted binding pockets. Combination mode diagrams of *CDKN2A* with irinotecan (**B**), lumacaftor (**C**), and nilotinib (**D**).

4. Discussion

DLBCL is a highly heterogeneous malignant tumor. Following the invention of rituximab, the prognosis of DLBCL patients has been significantly improved; however, 40% of patients still do not benefit from it. With the development of sequencing technology, there are new prognostic models for predicting the prognosis of DLBCL patients based on gene expression. Some of these models were widely used in the clinic, such as COO classification based on Cell Origin [5] and LymphGen Classifier based on the expression levels of some important genes [1]. Simultaneously, some exploratory studies that constructed prognostic models based on immune-related genes also achieved better results [22,23]. A prognostic model based on metabolism-related genes was constructed by He et al. [24]. Additionally, research was conducted to predict the prognosis of DLBCL patients based on the immune infiltration score [25]. However, none of these studies can fully explain the prognosis heterogeneity in DLBCL patients. Our study aims to

find a new prognostic model for DLBCL patients according to newly discovered mechanisms related to tumorigenesis and development.

Previous studies showed that regulated cell death (RCD) plays an important role in many diseases [26]. Apoptosis is the most intensively studied form of RCD, which involves the targets of almost all tumor treatment strategies [27]. As a relatively new discovery, ferroptosis has been widely evaluated in various tumors, such as melanoma, clear cell renal cell carcinoma, breast cancer, lung adenocarcinoma, hepatocellular carcinoma, etc [28–33]. Ferroptosis related genes, especially in DLBCL patients, can reliably predict the prognosis of patients and can also provide an assessment of the ibrutinib response [34]. As a new RCD, the role of cuproptosis in tumorigenesis and development is still unknown. At present, a few studies found that cuproptosis-related genes play an important role in some tumors, including melanoma, liver cancer, soft tissue sarcoma, and clear cell carcinoma [12,14,35,36]. This study was designed to investigate the predictive value of cuproptosis-related genes in DLBCL. This involved the construction of a prognostic model, CRS, based on 5 cuproptosis-related genes: *CDKN2A*, *DLAT*, *DLD*, *LIPT1*, and *MTF1*. The Kaplan-Meier survival analysis suggested that CRS is significantly associated with the OS of DLBCL patients in the presented training set ($p = 2.636 \times 10^{-7}$) and validation set ($p = 2.251 \times 10^{-4}$).

Our model can predict the prognosis of DLBCL patients as well as the models mentioned above. However, we found, for the first time, new biological functions and genes that affect the prognosis of DLBCL patients.

In the GSEA analysis of the high-risk and low-risk groups, the drug metabolism-other enzymes, mRNA transcription and late endosome to vacuole transport were significantly different. Other studies showed that these functions play a crucial role in the tumorigenesis and development of DLBCL or other lymphomas [37–41]. Our results further confirmed that these functions significantly impact the prognosis of DLBCL patients.

DLD and *DLAT* are dihydrolipoamide metabolism-related genes. One study found that *DLD* is related to the prognosis of certain tumors [42], while *DLAT* is rarely studied. Our study is the first to show that *DLD* and *DLAT* are associated with the prognosis of DLBCL patients. Dihydrolipoamide plays a crucial role in the tricarboxylic acid cycle, and therefore, we speculate that *DLD* and *DLAT* affect patient prognosis by participating in the energy metabolism of tumor cells. We will verify this hypothesis through further experiment *in vitro* and *in vivo*.

The melanoma patients with higher *LIPT1* expression showed longer OS than those with lower *LIPT1* expression after immunotherapy. In addition, compared with normal tissues, *LIPT1* was highly expressed in 18 tumor tissues including DLBCL, and its expression level was positively correlated with the expression of 8 immune checkpoint genes, especially PD-L1. Therefore, *LIPT1* is expected to become a regulator and predictor for immune checkpoint block therapy in a variety of tumors [14].

The products encoded by *MTF1* target genes can inhibit the intracellular stress response induced by radiotherapy, thus leading to radiotherapy resistance and promoting lymphoma drug resistance and progression [43]. Integrated with the findings of our study, *MTF1* is expected to be a therapeutic target for DLBCL patients in the future.

Cyclin dependent kinase inhibitor 2a (*CDKN2A*) is a member of the cell cycle dependent kinase inhibitor family. It is an important tumor suppressor gene in cells and has mutations in a variety of tumors. Dysregulation of MYC-CDKN2A-TP53 signaling pathway is common in NHL [44]. Recurrent mutations of *MYC*, *ID3*, *DDX3X*, and 9p21/*CDKN2A* homozygous deletion can often be detected in some high grade B-cell lymphoma-NOS (HGBCL-NOS) [45]. Interestingly, through the GEPIA database (http://gepia.cancer-pku.cn/) [46], it was found that the high expression of *CDKN2A* in various tumors, such as colon cancer/liver cancer, indicated poor prognosis. This study also found similar results in DLBCL, where higher expression of *CDKN2A* suggests a poorer prognosis, which is inconsistent with the role of its tumor suppressor gene. Therefore, it is believed that there are many unknown mechanisms in the transcription, translation, and epigenetic modification of *CDKN2A*. We hope to reveal these inconsistencies through further research.

It is worth mentioning that this study found that the high expression of *CDKN2A* is related to poor prognosis in DLBCL. Therefore, we conducted virtual screening of *CDKN2A* and 2115 compounds approved by FDA, and found three compounds with the lowest binding energy to *CDKN2A*: irinotecan, lumacaftor, and nilotinib. We hope to verify their binding to *CDKN2A* through subsequent cell and animal experiments, and further explore whether they can be used as targeted inhibitors to prolong the survival of DLBCL patients.

In summary, this study constructed a prognostic model that can predict the prognosis of DLBCL patients based on 5 cuproptosis-related genes, and preliminarily discussed the functional enrichment differences between patients with high and low risk scores. Finally, we screened out 3 compounds that may be used as targeted inhibitors for *CDKN2A* through molecular docking.

Supplementary Materials

The following supporting information can be found at: https://doi.org/10.35534/BG20240110002, Figure S1: To test the efficacy of the prognostic model in validation cohort, GSE181063. Figure S2: To predict the stability of this prognostic model.

Acknowledgments

We thank all colleagues involved in the study for their contributions.

Author Contributions

Conceptualization was supervised by L.G. Data curation was supervised by F.L. Investigation was supervised by J.C. Methodology was supervised by J.L. Project administration was supervised by X.Z. Resources were supervised by S.D. and S.L. Software was supervised by X.X. Supervision was led by L.G. Writing of the original draft was supervised by F.L. Writing of the review and editing were supervised by J.R.

Ethics Statement

The study was approved by the institutional review board of Xinqiao Hospital, Army Medical University, and performed in accordance with the principles expressed in the Declaration of Helsinki. All the subjects participating in the study provided written informed consent.

Informed Consent Statement

Not applicable.

Funding

This work was supported by the Chinese National Natural Science Foundation (Grant No. 81970162), Basic and Frontier Research Project of General Hospital of the Chinese People's Liberation Army Western Theater (Grant No. 2021XZYG-C44), Joint Project of Chongqing Health Commission and Science and Technology Bureau (2019QNXM021), and Joint Project of Chongqing Health Commission and Science and Technology Bureau (2022ZDXM025).

Declaration of Competing Interest

The authors declared no conflict of interests.

References

1. Wright GW, Huang DW, Phelan JD, Coulibaly ZA, Roulland S, Young RM, et al. A Probabilistic Classification Tool for Genetic Subtypes of Diffuse Large B Cell Lymphoma with Therapeutic Implications. *Cancer Cell* **2020**, *37*, 551–568.e14.
2. Tilly H, Vitolo U, Walewski J, da Silva MG, Shpilberg O, André M, et al. Diffuse large B-cell lymphoma (DLBCL): ESMO Clinical Practice Guidelines for diagnosis, treatment and follow-up. *Ann. Oncol.* **2012**, *23*, vii78–vii82.
3. Harkins RA, Chang A, Patel SP, Lee MJ, Goldstein JS, Merdan S, et al. Remaining challenges in predicting patient outcomes for diffuse large B-cell lymphoma. *Expert Rev. Hematol.* **2019**, *12*, 959–973.
4. Ruppert AS, Dixon JG, Salles GA, Wall A, Cunningham D, Poeschel V, et al. International prognostic indices in diffuse large B-cell lymphoma: a comparison of IPI, R-IPI, and NCCN-IPI. *Blood* **2020**, *135*, 2041–2048.
5. Chapuy B, Stewart C, Dunford AJ, Kim J, Kamburov A, Redd RA, et al. Molecular subtypes of diffuse large B cell lymphoma are associated with distinct pathogenic mechanisms and outcomes. *Nat. Med.* **2018**, *24*, 679–690.
6. Xu-Monette ZY, Li L, Byrd JC, Jabbar KJ, Manyam GC, de Winde CM, et al. Assessment of CD37 B-cell antigen and cell of origin significantly improves risk prediction in diffuse large B-cell lymphoma. *Blood* **2016**, *128*, 3083–3100.
7. Aukema SM, Siebert R, Schuuring E, van Imhoff GW, Kluin-Nelemans HC, Boerma E-J, et al. Double-hit B-cell lymphomas. *Blood* **2011**, *117*, 2319–2331.
8. Horn H, Ziepert M, Becher C, Barth TFE, Bernd H-W, Feller AC, et al. MYC status in concert with BCL2 and BCL6 expression predicts outcome in diffuse large B-cell lymphoma. *Blood* **2013**, *121*, 2253–2263.
9. Wang L, Li L-R, Young KH. New agents and regimens for diffuse large B cell lymphoma. *J. Hematol. Oncol.* **2020**, *13*, 1–23.

10. Tirado C, Chen W, García R, Kohlman K, Rao N. Genomic profiling using array comparative genomic hybridization define distinct subtypes of diffuse large b-cell lymphoma: a review of the literature. *J. Hematol. Oncol.* **2012**, *5*, 54–54.
11. Tsvetkov P, Coy S, Petrova B, Dreishpoon M, Verma A, Abdusamad M, et al. Copper induces cell death by targeting lipoylated TCA cycle proteins. *Science* **2022**, *375*, 1254–1261.
12. Zhang G, Sun J, Zhang X. A novel Cuproptosis-related LncRNA signature to predict prognosis in hepatocellular carcinoma. *Sci. Rep.* **2022**, *12*, 1–13.
13. Hu Q, Wang R, Ma H, Zhang Z, Xue Q. Cuproptosis predicts the risk and clinical outcomes of lung adenocarcinoma. *Front. Oncol.* **2022**, *12*, 922332.
14. Lv H, Liu X, Zeng X, Liu Y, Zhang C, Zhang Q, et al. Comprehensive Analysis of Cuproptosis-Related Genes in Immune Infiltration and Prognosis in Melanoma. *Front. Pharmacol.* **2022**, *13*, 930041.
15. Bishara AJ, Hittner JB. Testing the significance of a correlation with nonnormal data: Comparison of Pearson, Spearman, transformation, and resampling approaches.. *Psychol. Methods* **2012**, *17*, 399–417.
16. Chen X. Curve-Based Clustering Of Time Course Gene Expression Data Using Self-Organizing Maps. *J. Bioinform. Comput. Biol.* **2009**, *7*, 645–661.
17. Petushkova NA, Pyatnitskiy MA, Rudenko VA, Larina OV, Trifonova OP, Kisrieva JS, et al. Applying of Hierarchical Clustering to Analysis of Protein Patterns in the Human Cancer-Associated Liver. *PLOS ONE* **2014**, *9*, e103950.
18. Newman AM, Liu CL, Green MR, Gentles AJ, Feng W, Xu Y, et al. Robust enumeration of cell subsets from tissue expression profiles. *Nat. Methods* **2015**, *12*, 453–457.
19. Aleksander SA, Balhoff J, Carbon S, Cherry JM, Drabkin HJ, Ebert D, et al. The Gene Ontology knowledgebase in 2023. *Genetics* **2023**, *224*, iyad031.
20. Ashburner M, Ball CA, Blake JA, Botstein D, Butler H, Cherry JM, et al. Gene ontology: tool for the unification of biology. The Gene Ontology Consortium. *Nat. Genet*. **2000**, *25*, 25–29.
21. Kanehisa M, Goto S. KEGG: kyoto encyclopedia of genes and genomes. *Nucleic Acids Res.* **1999**, *28*, 27–30.
22. Mu S, Shi D, Ai L, Fan F, Peng F, Sun C, et al. International Prognostic Index-Based Immune Prognostic Model for Diffuse Large B-Cell Lymphoma. *Front. Immunol.* **2021**, *12*, 732006.
23. Liang X-J, Fu R-Y, Wang H-N, Yang J, Yao N, Liu X-D, et al. An Immune-Related Prognostic Classifier Is Associated with Diffuse Large B Cell Lymphoma Microenvironment. *J. Immunol. Res.* **2021**, *2021*, 1–26.
24. He J, Chen Z, Xue Q, Sun P, Wang Y, Zhu C, et al. Identification of molecular subtypes and a novel prognostic model of diffuse large B-cell lymphoma based on a metabolism-associated gene signature. *J. Transl. Med.* **2022**, *20*, 1–21.
25. Wang G, Qiu C, Zhang C, Hou S, Zhang Q. Construction of a DLBCL Prognostic Signature Based on Tumor Microenvironment. *Expert Rev. Hematol.* **2021**, *14*, 679–686.
26. Tang R, Xu J, Zhang B, Liu J, Liang C, Hua J, et al. Ferroptosis, necroptosis, and pyroptosis in anticancer immunity. *J. Hematol. Oncol.* **2020**, *13*, 1–18.
27. Qi X, Li Q, Che X, Wang Q, Wu G. Application of Regulatory Cell Death in Cancer: Based on Targeted Therapy and Immunotherapy. *Front. Immunol.* **2022**, *13*, 837293.
28. Ping S, Wang S, Zhao Y, He J, Li G, Li D, et al. Identification and validation of a ferroptosis-related gene signature for predicting survival in skin cutaneous melanoma. *Cancer Med.* **2022**, *11*, 3529–3541.
29. Jin J, Liu C, Yu S, Cai L, Sitrakiniaina A, Gu R, et al. A novel ferroptosis-related gene signature for prognostic prediction of patients with lung adenocarcinoma. *Aging* **2021**, *13*, 16144–16164.
30. Li H, Li L, Xue C, Huang R, Hu A, An X, et al. A Novel Ferroptosis-Related Gene Signature Predicts Overall Survival of Breast Cancer Patients. *Biology* **2021**, *10*, 151.
31. Wang S, Chen S, Ying Y, Ma X, Shen H, Li J, et al. Comprehensive Analysis of Ferroptosis Regulators With Regard to PD-L1 and Immune Infiltration in Clear Cell Renal Cell Carcinoma. *Front. Cell Dev. Biol.* **2021**, *9,* 12880.
32. Liang J-Y, Wang D-S, Lin H-C, Chen X-X, Yang H, Zheng Y, et al. A Novel Ferroptosis-related Gene Signature for Overall Survival Prediction in Patients with Hepatocellular Carcinoma. *Int. J. Biol. Sci.* **2020**, *16*, 2430–2441.
33. Zhuo S, Chen Z, Yang Y, Zhang J, Tang J, Yang K. Clinical and Biological Significances of a Ferroptosis-Related Gene Signature in Glioma. *Front. Oncol.* **2020**, *10,* 590861.
34. Weng J, Chen L, Liu H, Yang X-P, Huang L. Ferroptosis Markers Predict the Survival, Immune Infiltration, and Ibrutinib Resistance of Diffuse Large B cell Lymphoma. *Inflammation* **2022**, *45*, 1146–1161.
35. Han J, Hu Y, Liu S, Jiang J, Wang H. A Newly Established Cuproptosis-Associated Long Non-Coding RNA Signature for Predicting Prognosis and Indicating Immune Microenvironment Features in Soft Tissue Sarcoma. *J. Oncol.* **2022**, *2022*, 1–27.

36. Bian Z, Fan R, Xie L. A Novel Cuproptosis-Related Prognostic Gene Signature and Validation of Differential Expression in Clear Cell Renal Cell Carcinoma. *Genes* **2022**, *13*, 851.
37. Chen X, Lu T, Ding M, Cai Y, Yu Z, Zhou X, et al. Targeting YTHDF2 inhibits tumorigenesis of diffuse large B-cell lymphoma through ACER2-mediated ceramide catabolism. *J. Adv. Res.* 2023*, in press*.
38. Liu Y, Kimpara S, Hoang N-MM, Daenthanasanmak A, Li Y, Lu L, et al. EGR1-mediated metabolic reprogramming to oxidative phosphorylation contributes to ibrutinib resistance in B-cell lymphoma. *Blood* **2023**, *142*, 1879–1894.
39. Wimberger N, Ober F, Avar G, Grau M, Xu W, Lenz G, et al. Oncogene-induced MALT1 protease activity drives posttranscriptional gene expression in malignant lymphomas. *Blood* **2023**, *142*, 1985–2001.
40. Chen X, Lu T, Cai Y, Han Y, Ding M, Chu Y, et al. KIAA1429-mediated m6A modification of CHST11 promotes progression of diffuse large B-cell lymphoma by regulating Hippo–YAP pathway. *Cell. Mol. Biol. Lett.* **2023**, *28*, 1–29.
41. Lynch DT, Foucar K. Discrete vacuoles in lymphocytes as a subtle clue to mantle cell lymphoma. *Blood* **2016**, *127*, 3292–3292.
42. Shin D, Lee J, You JH, Kim D, Roh J-L. Dihydrolipoamide dehydrogenase regulates cystine deprivation-induced ferroptosis in head and neck cancer. *Redox Biol.* **2020**, *30*, 101418.
43. Tamura Y, Maruyama M, Mishima Y, Fujisawa H, Obata M, Kodama Y, et al. Predisposition to mouse thymic lymphomas in response to ionizing radiation depends on variant alleles encoding metal-responsive transcription factor-1 (Mtf-1). *Oncogene* **2004**, *24*, 399–406.
44. Trotman LC, Pandolfi PP. PTEN and p53: Who will get the upper hand? *Cancer Cell* **2003**, *3*, 97–99.
45. Ramis-Zaldivar JE, Gonzalez-Farré B, Balagué O, Celis V, Nadeu F, Salmerón-Villalobos JS, et al. Distinct molecular profile of IRF4-rearranged large B-cell lymphoma. *Blood* **2020**, *135*, 274–286.
46. Tang Z, Li C, Kang B, Gao G, Li C, Zhang Z. GEPIA: A web server for cancer and normal gene expression profiling and interactive analyses. *Nucleic Acids Res.* **2017**, *45*, W98–W10.